Engineering Analysis with Boundary Elements 26 (2002) 559–569

ENGINEERING ANALYSIS with BOUNDARY ELEMENTS

www.elsevier.com/locate/enganabound

An alternative method for degenerate scale problems in boundary element methods for the two-dimensional Laplace equation

J.T. Chen[a], C.F. Lee[a], I.L. Chen[b,*], J.H. Lin[c]

[a]Department of Harbor and River Engineering, National Taiwan Ocean University, P.O. Box 7-59, Keelung 202, Taiwan, ROC
[b]Department of Naval Architecture, Kaohsiung Institute of Marine Technology, Kaohsiung, Taiwan, ROC
[c]Department of Harbor and Coastal Engineering, China Engineering Consultants Inc., Taipei, Taiwan, ROC

Received 30 December 2001; revised 18 March 2002; accepted 4 April 2002

Abstract

The boundary integral equation approach has been shown to suffer a nonunique solution when the geometry is equal to a degenerate scale for a potential problem. In this paper, the degenerate scale problem in boundary element method for the two-dimensional Laplace equation is analytically studied in the continuous system by using degenerate kernels and Fourier series instead of using discrete system using circulants [Engng Anal. Bound. Elem. 25 (2001) 819]. For circular and multiply-connected domain problems, the rank-deficiency problem of the degenerate scale is solved by using the combined Helmholtz exterior integral equation formulation (CHEEF) concept. An additional constraint by collocating a point outside the domain is added to promote the rank of influence matrix. Two examples are shown to demonstrate the numerical instability using the singular integral equation for circular and annular domain problems. The CHEEF concept is successfully applied to overcome the degenerate scale and the error is suppressed in the numerical experiment.

Keywords: Boundary element method; Degenerate scale; Degenerate kernel; Combined Helmholtz exterior integral equation formulation concept; Fourier series

1. Introduction

Practical engineers [1] and academic researchers [2] have paid attention to applications of the boundary element method (BEM) in recent years. Although BEM is recognized as an acceptable tool, some pitfalls still exist, e.g. fictitious frequency and degenerate scale. A large amount of papers have been published on fictitious frequency [3–6], only a few researchers paid attention to the degenerate-scale problem. It is well known that rigid body motion test is employed to examine the singular matrices of strongly singular kernels and hypersingular kernels for the problems without degenerate boundaries. The singularity occurs physically and mathematically in the sense that the nonunique solution for the singular matrix includes a rigid body term for the interior Neumann problem. However, the influence matrix of the weakly singular kernel may be singular for the Dirichlet problem [7] when geometry is special. The nonunique solution is not physically realizable but results from the zero singular value of the influence matrix in the integral formulation. For example, the nonunique solution of a unit circle has been noted by Petrovsky [8] and by Jaswon and Symm [9]. The special geometry which results in a nonunique solution for a potential problem is called 'degenerate scale'. The term 'scale' stems from the fact that the numerical instability of a unit circle of radius 1 m (1 cm) disappears if the radius of 100 cm (0.01 m) is used in the BEM implementation. In real implementation, we need to avoid the number one for the circular radius using the normalized scale. The numerical difficulties due to nonuniqueness of solutions have been solved by the necessary and sufficient boundary integral equation (NSBIE) [10–13] and boundary contour method [14]. However, the boundary conditions in their cases are either the Dirichlet or the mixed type and must be constant along the circular boundary. Also, the degenerate scale of multiply-connected domain problems was discussed for the Laplace equation by Tomlinson et al. [15]. The degenerate scale for the multiply-connected biharmonic problems was also studied by Mitra and Das [16]. Chen et al. [17] studied

* Corresponding author. Tel.: +886-2-24622192x6140; fax: +886-2-24632375.
E-mail address: chen-i-Lin@kimo.com.tw (I.L. Chen).

0955-7997/02/$ - see front matter
PII: S0955-7997(02)00024-3

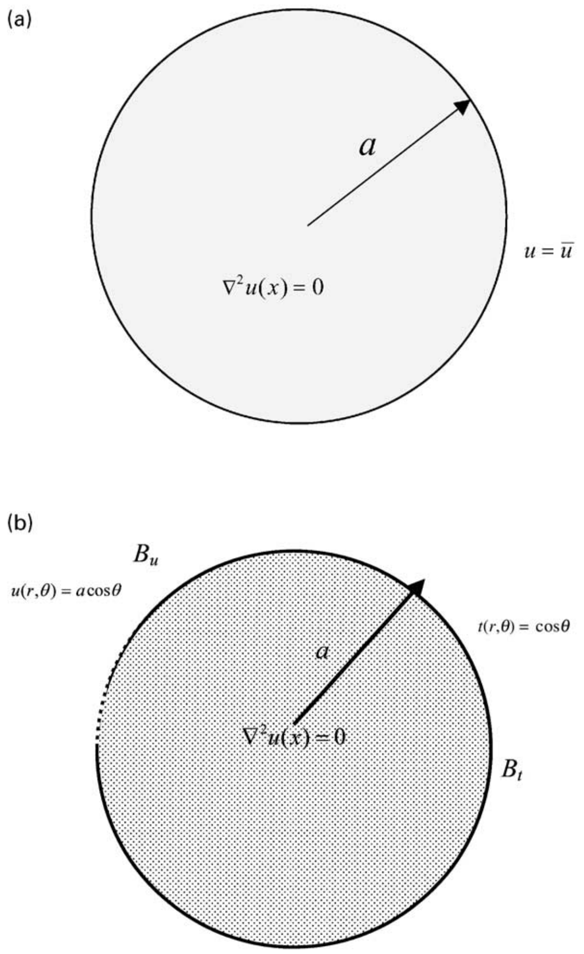

Fig. 1. (a) Potential problem with a Dirichlet boundary condition of a circular region. (b) Potential problem of a circular region with mixed boundary conditions.

the degenerate scale for the simply-connected and multiply-connected problems by using the degenerate kernels and circulants in a discrete system for circular and annular cases. Mathematically speaking, the singularity pattern distributed along a ring boundary resulting in a zero field introduces a degenerate scale. This concept was also extended to study the spurious eigenvalues for annular cavities by Chen et al. [18]. A similar application to the two-dimensional elasticity was addressed in Ref. [19]. A rigorous study was proposed mathematically by Kuhn [20] and Constanda [21,22] for the occurring mechanism of the degenerate scale. In the previous work [17], degenerate kernels and circulants were employed to study the occurring mechanism of degenerate scale in the discrete system of BEM. One alternative to treat the problem is to superimpose a rigid body term in the fundamental solution. Although the degenerate scale problem is circumvented for the special geometry, the degenerate scale moves to another size in reality. Also, hypersingular formulation can shift the zero eigenvalue in sacrifice of determining the Hadamard principal value. To seek a unified method for the degenerate scale problem is not trivial.

It is well known that rank deficiency is always encountered for the exterior and interior acoustic problems using BEM. Schenck [3] proposed a combined Helmholtz interior integral equation formulation (CHIEF) method, which is easy to implement by applying the integral equation on a number of points located outside the domain of interest. It is efficient to overcome the nonunique solution problem in case of fictitious frequency, but it still has some drawbacks since the chosen point may fail. How to determine the number of points and how to choose their positions was discussed by Chen et al. [6]. In a similar way, the combined Helmholtz exterior integral equation formulation (CHEEF) concept [23] has been employed to sort out the spurious eigenvalues by adding constraints from the points outside the domain in the multiple reciprocity BEM [24], real-part BEM [25] and imaginary-part BEM [26]. The CHEEF concept was successfully applied to filter out the spurious eigenvalues [23].

In this study, we will focus on the analytical investigation of phenomenon of degenerate scales in the BEM for the two-dimensional Laplace equation by using degenerate kernels and Fourier series expansion. Also, we will employ the CHEEF concept to overcome the nonunique solutions in numerical implementation. The optimum number for the collocating point will be studied analytically and verified numerically. By using the CHEEF technique, the missing constraint will be found. Two examples, a circular (simple connected) region and an annular (multi-connected) region, will be demonstrated for the degenerate scale problems.

2. Mathematical analysis of the degenerate scale for a circular problem

The governing equation for a potential problem is the Laplace equation as follows

$$\nabla^2 u(x) = 0, \qquad x \in D_{\mathrm{e}} \tag{1}$$

where ∇^2 is the Laplace operator, and D_{s} is the simply-connected domain of the problem. We consider the problem with a circular region of a radius a as shown in Fig. 1(a). For simplicity, the boundary condition is the Dirichlet type. Based on the boundary integral equation, a null field equation is considered as follows

$$0 = \int_B T(s,x)u(s)\mathrm{d}B(s) - \int_B U(s,x)t(s)\mathrm{d}B(s), \qquad x \in D_{\mathrm{e}} \tag{2}$$

where x is the field point, s is the source point, the kernel function, $U(s,x) = \ln r$, r is the distance between x and s, $T(s,x) = \partial U(s,x)/\partial n_s$, $t(s) = \partial u(s)/\partial n_s$ and D_{e} is the exterior domain of the problem. The null-field formulation can avoid the jump term since the collocation point is outside the domain. The degenerate kernel can distinguish the inside and outside points for the two-point fundamental solution. The same boundary integral equations can be obtained by either surface boundary integral equation or the null-field integral equation.

Based on Stanley's assumption for a simply-connected interior problem in the continuous system [27], the field solution can be expressed by

$$u(\rho,\theta) = a_0 + \sum_{n=1}^{\infty} (a_n\rho^n \cos(n\theta) + b_n\rho^n \sin(n\theta)); \quad 0 < \rho < a, \quad 0 \le \theta < 2\pi \tag{3}$$

By setting $\rho = a$, the field solution u reduces to the boundary data, where a is the radius of domain. The secondary boundary quantity along the circular boundary can be expanded in terms of Fourier series,

$$t(a,\theta) = p_0 + \sum_{n=1}^{\infty} (p_n \cos(n\theta) + q_n \sin(n\theta)), \quad 0 < \theta < 2\pi \tag{4}$$

Based on the separate properties for the kernels, the kernel functions in Eq. (2) can be expanded into degenerate forms as shown below [25,28–30]

$$U(s,x) = \begin{cases} U^{\mathrm{i}}(R,\theta;\rho,\phi) = \ln R - \sum_{m=1}^{\infty} \frac{1}{m}\left(\frac{\rho}{R}\right)^m \cos(m(\theta-\phi)), & R > \rho \\ U^{\mathrm{e}}(R,\theta;\rho,\phi) = \ln \rho - \sum_{m=1}^{\infty} \frac{1}{m}\left(\frac{R}{\rho}\right)^m \cos(m(\theta-\phi)), & \rho > R \end{cases} \tag{5}$$

$$T(s,x) = \begin{cases} T^{\mathrm{i}}(R,\theta;\rho,\phi) = \frac{1}{R} + \sum_{m=1}^{\infty} \left(\frac{\rho^m}{R^{m+1}}\right) \cos(m(\theta-\phi)), & R > \rho \\ T^{\mathrm{e}}(R,\theta;\rho,\phi) = -\sum_{m=1}^{\infty} \left(\frac{R^{m-1}}{\rho^m}\right) \cos(m(\theta-\phi)), & \rho > R \end{cases} \tag{6}$$

where the superscripts 'i' and 'e' denotes the interior domain ($R > \rho$) and the exterior domain ($\rho > R$), (ρ,ϕ) and (R,θ) are the polar coordinates for x and s, respectively. It must be noted that the superscripts i and e are used for the interior and exterior problems to avoid the source terms, respectively. Substitution of the T^{e} and U^{e} kernels of the degenerate forms of Eqs. (5) and (6), and the boundary densities u, t of Eqs. (3) and (4) into Eq. (2) gives

$$\begin{aligned} &\int_0^{2\pi} \left[-\sum_{m=1}^{\infty} \frac{a^{m-1}}{\rho^m} \cos(m(\theta-\phi)) \right] \left[a_0 + \sum_{n=1}^{\infty} (a_n a^n \cos(n\theta) + b_n a^n \sin(n\theta)) \right] a \, \mathrm{d}\theta \\ &= \int_0^{2\pi} \left[\ln\rho - \sum_{m=1}^{\infty} \frac{1}{m}\left(\frac{a}{\rho}\right)^m \cos(m(\theta-\phi)) \right] \left[p_0 + \sum_{n=1}^{\infty} (p_n \cos(n\theta) + q_n \sin(n\theta)) \right] a \, \mathrm{d}\theta. \end{aligned} \tag{7}$$

By using the orthogonal properties of Fourier bases, Eq. (7) can be formulated to

$$\begin{aligned} &\pi a(2p_0 \ln\rho - 0{\cdot}a_0) \\ &+ \pi a \sum_{n=1}^{\infty} \left(\frac{R}{\rho}\right)^n \left[a_n a^{n-1} - \frac{p_n}{n} \right] \cos(n\phi) \\ &+ \pi a \sum_{n=1}^{\infty} \left(\frac{R}{\rho}\right)^n \left[b_n a^{n-1} - \frac{q_n}{n} \right] \sin(n\phi) = 0. \end{aligned} \tag{8}$$

Since the collocation point (a^+,ϕ) is arbitrary along the circular boundary ($0 \le \phi < 2\pi$), we have

$$p_0 = \frac{0{\cdot}a_0}{2\ln a^+}, \qquad p_n = na^{n-1}a_n, \quad q_n = na^{n-1}b_n, \quad n = 1,2,3,\ldots \tag{9}$$

When the radius a is equal to one, the coefficient of p_0 in Eq. (9) is zero division by zero. It indicates that the solution is nonunique when a is the specific magnitude which is equal to the degenerate scale. In this case, we can choose an exterior point to solve the degenerate scale problem by using the CHEEF technique.

By choosing an exterior point x_1 with the polar coordinate of (r_1,ϕ_1), substitution of the T^{e} and U^{e} kernels of degenerate forms of Eqs. (5) and (6), and the boundary densities u, t of Eqs. (3) and (4) into Eq. (2), gives

$$\begin{aligned} &\int_0^{2\pi} \left[-\sum_{m=1}^{\infty} \frac{a^{m-1}}{r_1^m} \cos(m(\theta-\phi_1)) \right] \left[a_0 + \sum_{n=1}^{\infty} (a_n a^n \cos(n\theta) + b_n a^n \sin(n\theta)) \right] a \, \mathrm{d}\theta \\ &= \int_0^{2\pi} \left[\ln r_1 - \sum_{m=1}^{\infty} \frac{1}{m}\left(\frac{a}{r_1}\right)^m \cos(m(\theta-\phi_1)) \right] \left[p_0 + \sum_{n=1}^{\infty} (p_n \cos(n\theta) + q_n \sin(n\theta)) \right] a \, \mathrm{d}\theta. \end{aligned} \tag{10}$$

Eq. (10) can be formulated to

$$\begin{aligned} &\pi a(2p_0 \ln r_1 - 0{\cdot}a_0) \\ &+ \pi a \sum_{n=1}^{\infty} \left(\frac{a}{r_1}\right)^n \left[a_n a^{n-1} - \frac{p_n}{n} \right] \cos(n\phi) \\ &+ \pi a \sum_{n=1}^{\infty} \left(\frac{a}{r_1}\right)^n \left[b_n a^{n-1} - \frac{q_n}{n} \right] \sin(n\phi) = 0. \end{aligned} \tag{11}$$

When the radius of the collocating point is greater than one ($r_1 > 1$), the coefficient of p_0, $\ln r_1$, is not zero in Eq. (11). Therefore, we can avoid the degenerate scale in the circular domain problems by using the CHEEF technique.

3. Mathematical analysis of the degenerate scale for an annular problem

An annular domain composed of two concentric circles is shown in Fig. 2, and the governing equation is

$$\nabla^2 u(x) = 0, \qquad x \in D_{\mathrm{m}} \tag{12}$$

where D_{m} is the multiply-connected domain and the well-posed boundary conditions are

$$u(x) = u_1 \text{ or } t(x) = t_1, \qquad x \in B_1\ (r = R_1) \tag{13}$$

$$u(x) = u_2 \text{ or } t(x) = t_2, \qquad x \in B_2\ (r = R_2) \tag{14}$$

For the multiply-connected problems, Stanley's assumption for the solution of a multiply-connected interior problem gives [27]

$$u(r,\theta) = a_0 + b_0 \ln r + \sum_{n=1}^{\infty} [(a_n r^n + b_n r^{-n})\cos(n\theta) + (c_n r^n + d_n r^{-n})\sin(n\theta)]; \tag{15}$$

$R_1 \le r \le R_2,\ \ 0 \le \theta < 2\pi$

where R_1 and R_2 are the inner and the outer radii, respectively, a_0, b_0, a_n, b_n, c_n and d_n are the coefficients. Substituting R_1 or R_2 for r into Eq. (15), we have the boundary data

$$\begin{aligned} u_1 &= a_0 + b_0 \ln R_1 + \sum_{n=1}^{\infty} [(a_n R_1^n + b_n R_1^{-n})\cos(n\theta) \\ &\quad + (c_n R_1^n + d_n R_1^{-n})\sin(n\theta)] \\ &= \bar{a}_0 + \sum_{n=1}^{\infty} [\bar{a}_n \cos(n\theta) + \bar{b}_n \sin(n\theta)], \end{aligned} \tag{16}$$

$$\begin{aligned} u_2 &= a_0 + b_0 \ln R_2 + \sum_{n=1}^{\infty} [(a_n R_2^n + b_n R_2^{-n})\cos(n\theta) \\ &\quad + (c_n R_2^n + d_n R_2^{-n})\sin(n\theta)] \\ &= \bar{c}_0 + \sum_{n=1}^{\infty} [\bar{c}_n \cos(n\theta) + \bar{d}_n \sin(n\theta)], \end{aligned} \tag{17}$$

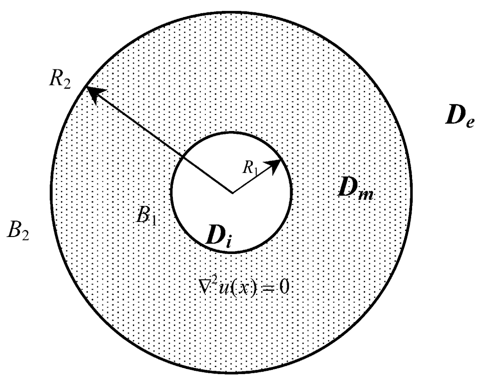

Fig. 2. Potential problem of an annular region.

where u_1 and u_2 are the boundary data for the primary field as shown in Eqs. (13) and (14). The boundary data for the secondary field can be expanded in Fourier series,

$$t_1(x) = p_0 + \sum_{n=1}^{\infty} (p_n \cos(n\theta) + q_n \sin(n\theta), \qquad x \in B_1 \tag{18}$$

$$t_2(x) = v_0 + \sum_{n=1}^{\infty} (v_n \cos(n\theta) + w_n \sin(n\theta)), \qquad x \in B_2 \tag{19}$$

where p_n, q_n, v_n and w_n are the Fourier coefficients. The exterior domain includes the inner domain D_{i} and the outer domain D_{e} for the multiply-connected problem as shown in Fig. 2. The null-field equation is

$$\begin{aligned} 0 &= \int_{B_1} T(s,x)u_1(s)\mathrm{d}B(s) - \int_{B_1} U(s,x)t_1(s)\mathrm{d}B_1(s) \\ &\quad + \int_{B_2} T(s,x)u_2(s)\mathrm{d}B(s) - \int_{B_2} U(s,x)t_2(s)\mathrm{d}B_2(s), \end{aligned} \tag{20}$$

$x \in D^{\mathrm{e}}$

where $t_1(s) = \partial u_1(s)/\partial n_s$ and $t_2 = \partial u_2(s)/\partial n_s$.

By moving the point x to the boundary B_1^-, where u_1 and u_2 are specified, t_1 and t_2 are unknown, substitution of the T^{i} and U^{i} kernels of degenerate forms in Eqs. (5) and (6), and the boundary densities u, t of Eqs. (16)–(19) into Eq. (20), gives

$$\begin{aligned} &\int_0^{2\pi} \left[\frac{1}{R_1} + \sum_{m=1}^{\infty} \frac{\rho^m}{R_1^{m+1}} \cos(m(\theta-\phi)) \right] \\ &\quad \left[\bar{a}_0 + \sum_{n=1}^{\infty} (\bar{a}_n \cos(n\theta) + \bar{b}_n \sin(n\theta)) \right] R_1\, \mathrm{d}\theta \\ &\quad - \int_0^{2\pi} \left[\ln R_1 - \sum_{m=1}^{\infty} \frac{1}{m} \left(\frac{\rho}{R_1} \right)^m \cos(m(\theta-\phi)) \right] \\ &\quad \left[p_0 + \sum_{n=1}^{\infty} (p_n \cos(n\theta) + q_n \sin(n\theta)) \right] R_1\, \mathrm{d}\theta \\ &\quad + \int_0^{2\pi} \left[\frac{1}{R_2} + \sum_{m=1}^{\infty} \frac{\rho^m}{R_2^{m+1}} \cos(m(\theta-\phi)) \right] \\ &\quad \left[\bar{c}_0 + \sum_{n=1}^{\infty} (\bar{c}_n \cos(n\theta) + \bar{d}_n \sin(n\theta)) \right] R_2\, \mathrm{d}\theta \\ &\quad - \int_0^{2\pi} \left[\ln R_2 - \sum_{m=1}^{\infty} \frac{1}{m} \left(\frac{\rho}{R_2} \right)^m \cos(m(\theta-\phi)) \right] \\ &\quad \left[v_0 + \sum_{n=1}^{\infty} (v_n \cos(n\theta) + w_n \sin(n\theta)) \right] R_2\, \mathrm{d}\theta = 0. \end{aligned} \tag{21}$$

By approaching the collocation point x to (R_1^-, ϕ), Eq. (21)

can be formulated to

$$\pi R_1\left[\frac{2\bar{a}_0}{R_1}+\sum_{n=1}^{\infty}\frac{(R_1^-)^n}{R_1^{n+1}}(\bar{a}_n\cos(n\phi)+\bar{b}_n\sin(n\phi))\right]-\pi R_1$$
$$\left[2p_0\ln R_1-\sum_{n=1}^{\infty}\left(\frac{R_1^-}{R_1}\right)^n\left[\frac{p_n}{n}\cos(n\phi)+\frac{q_n}{n}\sin(n\phi)\right]\right]$$
$$+\pi R_2\left[\frac{2\bar{c}_0}{R_2}+\sum_{n=1}^{\infty}\frac{(R_1^-)^n}{R_2^{n+1}}(\bar{c}_n\cos(n\phi)+\bar{d}_n\sin(n\phi))\right]$$
$$-\pi R_2$$
$$\left[2v_0\ln R_2-\sum_{n=1}^{\infty}\left(\frac{R_1^-}{R_2}\right)^n\left[\frac{v_n}{n}\cos(n\phi)+\frac{w_n}{n}\sin(n\phi)\right]\right]$$
$$=0. \tag{22}$$

By moving the point x to the boundary B_2^+, where u_1 and u_2 are specified, t_1 and t_2 are unknown, substitution of the T^{e} and U^{e} kernels of degenerate forms in Eqs. (5) and (6), and the boundary densities u, t of Eqs. (16)–(19) into Eq. (20), gives

$$\int_0^{2\pi}\left[-\sum_{m=1}^{\infty}\frac{R_1^{m-1}}{\rho^m}\cos(m(\theta-\phi))\right]$$
$$\left[\bar{a}_0+\sum_{n=1}^{\infty}\bar{a}_n\cos(n\theta)+\bar{b}_n\sin(n\theta)\right]R_1\,\mathrm{d}\theta$$
$$-\int_0^{2\pi}\left[\ln\rho-\sum_{m=1}^{\infty}\frac{1}{m}\left(\frac{R_1}{\rho}\right)^m\cos(m(\theta-\phi))\right]$$
$$\left[p_0+\sum_{n=1}^{\infty}p_n\cos(n\theta)+q_n\sin(n\theta)\right]R_1\,\mathrm{d}\theta$$
$$+\int_0^{2\pi}\left[-\sum_{m=1}^{\infty}\frac{R_2^{m-1}}{\rho^m}\cos(m(\theta-\phi))\right]$$
$$\left[\bar{c}_0+\sum_{n=1}^{\infty}\bar{c}_n\cos(n\theta)+\bar{d}_n\sin(n\theta)\right]R_2\,\mathrm{d}\theta$$
$$-\int_0^{2\pi}\left[\ln\rho-\sum_{m=1}^{\infty}\frac{1}{m}\left(\frac{R_2}{\rho}\right)^m\cos(m(\theta-\phi))\right]$$
$$\times\left[v_0+\sum_{n=1}^{\infty}v_n\cos(n\theta)+w_n\sin(n\theta)\right]R_2\,\mathrm{d}\theta=0. \tag{23}$$

By approaching the collocation point x to (R_2^+,ϕ), Eq. (23) can be formulated to

$$\pi R_1\left[0\cdot\bar{a}_0-\sum_{n=1}^{\infty}\frac{R_1^{n-1}}{(R_2^+)^n}(\bar{a}_n\cos(n\phi)+\bar{b}_n\sin(n\phi))\right]-\pi R_1$$
$$\left[2p_0\ln R_2^+-\sum_{n=1}^{\infty}\left(\frac{R_1}{R_2^+}\right)^n\left[\frac{p_n}{n}\cos(n\phi)+\frac{q_n}{n}\sin(n\phi)\right]\right]$$
$$+\pi R_2\left[0\cdot\bar{c}_0-\sum_{n=1}^{\infty}\frac{R_2^{n-1}}{(R_2^+)^n}(\bar{c}_n\cos(n\phi)+\bar{d}_n\sin(n\phi))\right]$$
$$-\pi R_2$$
$$\left[2v_0\ln R_2^+-\sum_{n=1}^{\infty}\left(\frac{R_2}{R_2^+}\right)^n\left[\frac{v_n}{n}\cos(n\phi)+\frac{w_n}{n}\sin(n\phi)\right]\right]$$
$$=0. \tag{24}$$

For this annular problem subject to Dirichlet boundary condition, u_1 and u_2 are specified. The normal fluxes, t_1 and t_2, are unknown. According to Eqs. (22) and (24), we can determine the coefficients of p_0 and v_0 by

$$p_0=\frac{(\bar{a}_0+\bar{c}_0)\ln R_2^+}{R_1(\ln R_1-\ln R_2)\ln R_2^+},$$
$$v_0=\frac{(\bar{a}_0+\bar{c}_0)\ln R_2^+}{R_2(\ln R_2-\ln R_1)\ln R_2^+}. \tag{25}$$

No matter what the value of the inner radius R_1 is, it does not contribute any singularity. However, the outer radius R_2 of unit length causes the failure in determining the coefficients of p_0 and v_0 in Eq. (25). Therefore, the degenerate scale occurs when the value of outer radius is one.

In order to solve the ill-posed problem, we may try either a point x_1 in the domain D_{i}, or a point x_2 in the domain D_{e} to solve the degenerate scale problem. How to select the collocation point to overcome the degenerate scale by using the CHIEF concept will be investigated as follows.

By choosing a point x_1 with the polar coordinate (r_1,ϕ_1) in the domain D_{i} as shown in Fig. 3(a), substitution of the degenerate kernels of T^{i}, U^{i} of Eqs. (5) and (6), and the

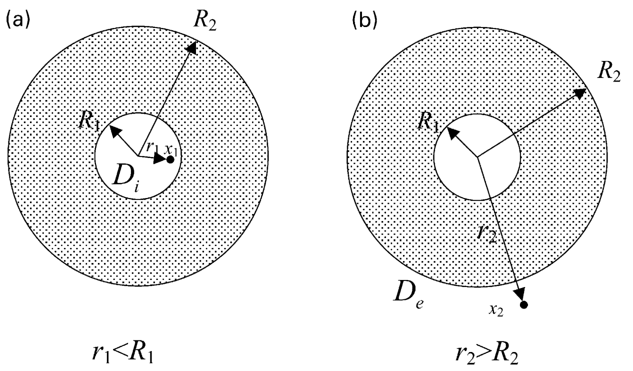

Fig. 3. Interior (CHIEF) point and exterior (CHEEF) point.

boundary densities u, t of Eqs. (16)–(19) into Eq. (20), gives

$$\int_0^{2\pi}\left[\frac{1}{R_1}+\sum_{m=1}^{\infty}\frac{r_1^m}{R_1^{m+1}}\cos(m(\theta-\phi_1))\right]\left[\bar{a}_0+\sum_{n=1}^{\infty}(\bar{a}_n\cos(n\theta)+\bar{b}_n\sin(n\theta))\right]R_1\,\mathrm{d}\theta$$
$$-\int_0^{2\pi}\left[\ln R_1-\sum_{m=1}^{\infty}\frac{1}{m}\left(\frac{r_1}{R_1}\right)^m\cos(m(\theta-\phi_1))\right]\left[p_0+\sum_{n=1}^{\infty}(p_n\cos(n\theta)+q_n\sin(n\theta))\right]R_1\,\mathrm{d}\theta$$
$$+\int_0^{2\pi}\left[\frac{1}{R_2}+\sum_{m=1}^{\infty}\frac{r_1^m}{R_2^{m+1}}\cos(m(\theta-\phi_1))\right]\left[\bar{c}_0+\sum_{n=1}^{\infty}(\bar{c}_n\cos(n\theta)+\bar{d}_n\sin(n\theta))\right]R_2\,\mathrm{d}\theta$$
$$-\int_0^{2\pi}\left[\ln R_2-\sum_{m=1}^{\infty}\frac{1}{m}\left(\frac{r_1}{R_2}\right)^m\cos(m(\theta-\phi_1))\right]\left[v_0+\sum_{n=1}^{\infty}(v_n\cos(n\theta)+w_n\sin(n\theta))\right]R_2\,\mathrm{d}\theta=0. \quad (26)$$

Eq. (26) can be formulated to

$$\pi R_1\left[\frac{2\bar{a}_0}{R_1}+\sum_{n=1}^{\infty}\frac{r_1^n}{R_1^{n+1}}(\bar{a}_n\cos(n\phi_1)+\bar{b}_n\sin(n\phi_1))\right]-\pi R_1\left[2p_0\ln R_1-\sum_{n=1}^{\infty}\left(\frac{r_1}{R_1}\right)^n\left[\frac{p_n}{n}\cos(n\phi_1)+\frac{q_n}{n}\sin(n\phi_1)\right]\right]$$
$$+\pi R_2\left[\frac{2\bar{c}_0}{R_2}+\sum_{n=1}^{\infty}\frac{r_1^n}{R_2^{n+1}}(\bar{c}_n\cos(n\phi_1)+\bar{d}_n\sin(n\phi_1))\right]-\pi R_2\left[2v_0\ln R_2-\sum_{n=1}^{\infty}\left(\frac{r_1}{R_2}\right)^n\left[\frac{v_n}{n}\cos(n\phi_1)+\frac{w_n}{n}\sin(n\phi_1)\right]\right]=0. \quad (27)$$

When the value of outer radius R_2 is equal to one, the coefficient of v_0 cannot be determined in Eq. (27). Therefore, CHEEF concept fails to deal with the degenerate scale problems if a point is chosen inside the inner circle.

By choosing another point x_2 with the polar coordinate (r_2,ϕ_2) in the D_e domain as shown in Fig. 3(b), substitution of the degenerate kernels of T^e, U^e in Eqs. (5) and (6), and the boundary densities u, t of Eqs. (16)–(19) into Eq. (20) gives

$$\int_0^{2\pi}\left[-\sum_{m=1}^{\infty}\frac{R_1^{m-1}}{r_2^m}\cos(m(\theta-\phi_2))\right]\left[\bar{a}_0+\sum_{n=1}^{\infty}\bar{a}_n\cos(n\theta)+\bar{b}_n\sin(n\theta)\right]R_1\,\mathrm{d}\theta$$
$$-\int_0^{2\pi}\left[\ln r_2-\sum_{m=1}^{\infty}\frac{1}{m}\left(\frac{R_1}{r_2}\right)^m\cos(m(\theta-\phi_2))\right]\left[p_0+\sum_{n=1}^{\infty}p_n\cos(n\theta)+q_n\sin(n\theta)\right]R_1\,\mathrm{d}\theta$$
$$+\int_0^{2\pi}\left[-\sum_{m=1}^{\infty}\frac{R_2^{m-1}}{r_2^m}\cos(m(\theta-\phi_2))\right]\left[\bar{c}_0+\sum_{n=1}^{\infty}\bar{c}_n\cos(n\theta)+\bar{d}_n\sin(n\theta)\right]R_2\,\mathrm{d}\theta$$
$$-\int_0^{2\pi}\left[\ln r_2-\sum_{m=1}^{\infty}\frac{1}{m}\left(\frac{R_2}{r_2}\right)^m\cos(m(\theta-\phi_2))\right]\times\left[v_0+\sum_{n=1}^{\infty}v_n\cos(n\theta)+w_n\sin(n\theta)\right]R_2\,\mathrm{d}\theta=0. \quad (28)$$

Eq. (28) can be formulated to

$$\pi R_1\left[0\cdot\bar{a}_0-\sum_{n=1}^{N}\frac{R_1^{n-1}}{r_2^n}(\bar{a}_n\cos(n\phi_2)+\bar{b}_n\sin(n\phi_2))\right]-\pi R_1\left[2p_0\ln r_2-\sum_{n=1}^{\infty}\left(\frac{R_1}{r_2}\right)^n\left[\frac{p_n}{n}\cos(n\phi_2)+\frac{q_n}{n}\sin(n\phi_2)\right]\right]$$
$$+\pi R_2\left[0\cdot\bar{c}_0-\sum_{n=1}^{\infty}\frac{R_2^{n-1}}{r_2^n}(\bar{c}_n\cos(n\phi_2)+\bar{d}_n\sin(n\phi_2))\right]-\pi R_2\left[2v_0\ln r_2-\sum_{n=1}^{\infty}\left(\frac{R_2}{r_2}\right)^n\left[\frac{v_n}{n}\cos(n\phi_2)+\frac{w_n}{n}\sin(n\phi_2)\right]\right]=0. \quad (29)$$

By collocating x_2 point outside the outer circle boundary ($r_2>1$) the coefficients of p_0 and v_0 can be easily determined in Eq. (29), even though the value of outer radius R_2 is one. Therefore, the degenerate scale can be overcome in the annular problems by using the CHEEF point in the D_e domain.

Table 1
Numerical results for the potential problem with a circular region ($a = 2$, normal scale)

θ (°)	Analytical solution		Singular equation		Hypersingular equation		CHEEF method point: (5, 0)	
	u	t	u	t	u	t	u	t
121.5	−1.045	−0.522	−1.045	−0.516 (1.1)	−1.045	−0.499 (4.4)	−1.045	−0.512 (1.9)
148.5	−1.705	−0.852	−1.705	−0.850 (0.2)	−1.705	−0.848 (0.4)	−1.705	−0.849 (0.4)
193.5	−1.994	−0.972	−1.892 (5.1)	−0.972	−1.894 (5.0)	−0.972	−1.912 (4.1)	−0.972
220.5	−1.521	−0.760	−1.481 (2.6)	−0.760	−1.504 (1.1)	−0.760	−1.512 (0.6)	−0.760

Data in parentheses denotes error, %.

4. Numerical examples for the circular and annular cases

4.1. Circular case

We consider the interior potential problem of a circular domain (Fig. 1(b)) with the mixed type condition as follows

$$t(r,\theta) = \cos(\theta); \qquad r = a, \quad -\pi < \theta < \frac{1}{2}\pi, \quad (r,\theta) \in B_t \tag{30}$$

$$u(r,\theta) = a\cos(\theta); \qquad r = a, \quad \frac{1}{2}\pi < \theta < \pi, \quad (r,\theta) \in B_u \tag{31}$$

where B_u and B_t are the specified Dirichlet and Neumann boundaries. In the BEM mesh, 10 elements are distributed uniformly on B_t and 10 elements on B_u. The analytical solutions are $u(r,\theta) = a\cos(\theta)$ and $t(r,\theta) = \cos(\theta)$. The numerical results are shown in Tables 1 and 2. The degenerate scale occurs numerically at $a = 1.012$ [17] instead of the analytical value $a = 1$. It is found that the errors of three approaches, *UT* equation, hypersingular formulation for the *LM* equation and CHEEF concept, are less than 5% error in case of the normal scale in Fig. 4. However, it results in a great error of 25% by using the singular formulation (UT equation) in case of the degenerate scale in Fig. 5. Although the hypersingular formulation (LM equation) can yield the solution more accurately (5.7%) as shown in Table 2 and Fig. 5, the regularization technique is required for hypersingularity. By employing the CHEEF concept free of the hypersingularity, the error reduces to a smaller one of 0.2% as shown in Fig. 5. Only one CHEEF point is required to solve the problem more accurately (0.2%) since rank is deficient by one in the degenerate scale problems. For comparison, the result of singular equation by adding a rigid body motion is also shown in Table 2.

4.2. Annular case

Given an annular problem with the mixed boundary conditions as follows

$$u_1(x) = 100, \qquad x \in B_1 \tag{32}$$

$$t_2(x) = \frac{100}{R_2 \ln \dfrac{R_1}{R_2}}, \qquad x \in B_2 \tag{33}$$

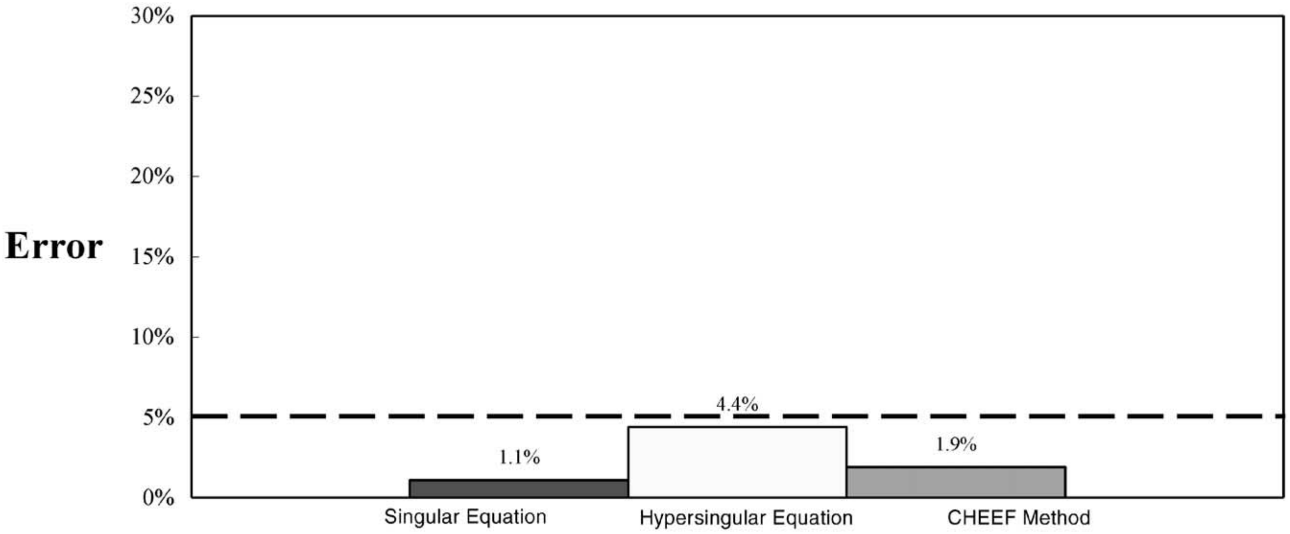

Fig. 4. The error distribution for the potential problem with a circular region ($a = 2$, normal scale).

Table 2
Numerical results for the potential problem with a circular region ($a = 1.012$, degenerate scale)

θ (°)	Analytical solution		Singular equation		Hypersingular equation		Singular equation + rigid body motion		CHEEF method point: (5, 0)	
	u	t	u	t	u	t	u	t	u	t
121.5	−0.529	−0.522	−0.529	−0.392 (25)	−0.529	−0.499 (5.7)	−0.529	−0.516 (1.15)	−0.529	−0.521 (0.2)
148.5	−0.863	−0.852	−0.863	−0.726 (14.8)	−0.863	−0.848 (1.7)	−0.863	−0.850 (0.23)	−0.863	−0.849 (0.35)
193.5	−0.984	−0.972	−1.025 (4.2)	−0.972	−0.958 (2.6)	−0.972	−0.984 (0.00)	−0.972	−0.977 (0.7)	−0.972
220.5	−0.769	−0.760	−0.856 (11.3)	−0.760	−0.761 (1.04)	−0.760	−0.750 (2.47)	−0.760	−0.761 (1.04)	−0.760

Data in parentheses denotes error, %.

the analytical solution is [31]

$$u(r) = u_2 + \frac{\ln \frac{r}{R_2}}{\ln \frac{R_1}{R_2}}(u_1 - u_2), \qquad R_1 \le r \le R_2 \tag{34}$$

where $2R_1 = R_2$ and u_2 is the potential on B_2. The same number of elements on the internal and exterior circles are adopted. The results are listed in Table 3, where $2N$ denotes the number of elements. Since the problem is axisymmetric, the observed point for the error can be at any place of the circular boundary. Also the point error and average error are the same. In Table 3, we find that the error of u_2 and t_1 are very large in the case of the degenerate scale ($R_2 = 1$) using the singular formulation. The hypersingular equation fails to solve the problem as predicted theoretically by Chen et al. [17]. However, we can obtain the more accurate results by choosing a point outside the outer circle. It is found that a point inside the inner circle cannot reduce the error as shown in Table 4 as predicted analytically. The additional invalid CHIEF point does not improve the results but deteriorates the solution since the weighting of the effective point is reduced. By choosing a CHEEF point outside the outer circle, the error of t_1 is suppressed to a smaller value for the degenerate case of $R_2 = 1$ as shown in Fig. 6. Also, the results by adding a rigid body motion [17] and NSBIE method [10] are compared with the present results in Table 3. Numerical instability is efficiently suppressed by using the CHEEF concept in Table 4. The CHIEF point inside the inner circle boundary cannot improve the accuracy. However, one exterior CHEEF point can yield good results. An extra exterior point does not contribute any more since rank is deficient by only one as shown in Table 4.

5. Conclusions

In this paper, we have proved why degenerate scale is embedded in the BEM for the two-dimensional Laplace equation by using the degenerate kernels and Fourier series. The proof of degenerate scale is not for a general geometry but for two special cases. For the simply-connected domain of a circular case with the Dirichlet boundary condition, the radius of unit length is a degenerate scale if the singular equation is used. In order to overcome the problem, CHEEF technique was adopted. This method is more systematic than the addition of a rigid body mode since the latter method introduces another degenerate scale. No new degenerate scale occurs by using the CHEEF technique. For the multiply-connected domain with an annular region, outer radius of unit length results in a nonunique solution. It is found that only one CHEEF point is required to deal with the problem efficiently. It is expected that no failure point outside the outer circular boundary be encountered since

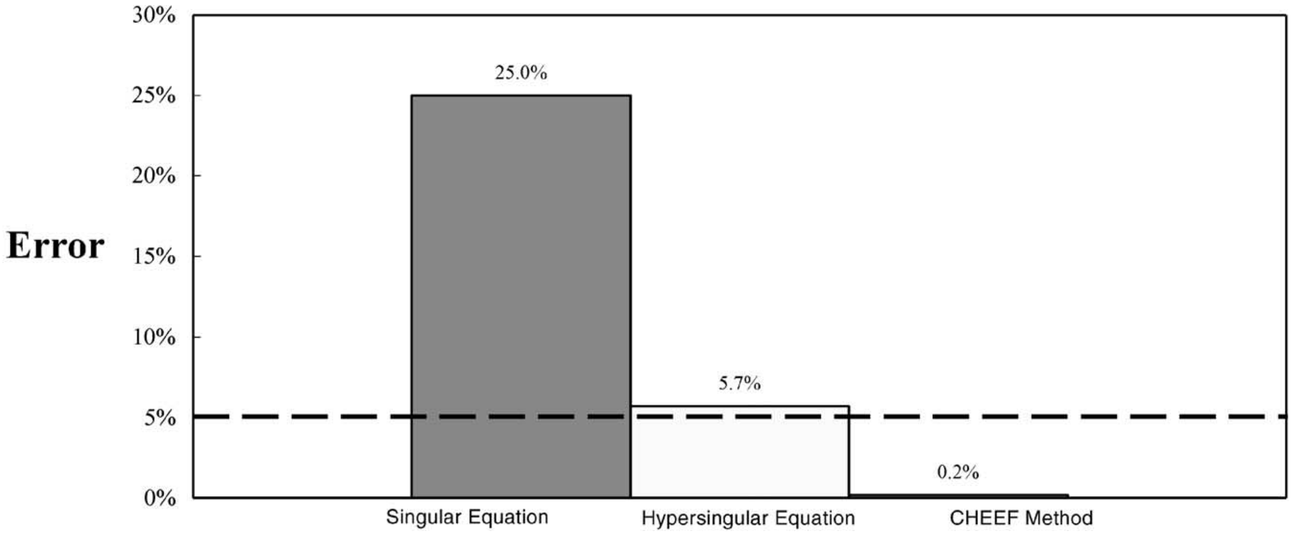

Fig. 5. The error distribution for the potential problem with a circular region ($a = 1.012$, degenerate scale).

Table 3
Numerical results for the potential problem with a multiply connected region by using the rigid body motion method and NSBIE method

$2N$	R_2	Analytical solution		Singular equation ($U = \ln r$)		Singular equation ($U = \ln r + 10$)		Hypersingular equation ($U = \ln r$)		Hypersingular equation ($U = \ln r + 10$)		NSBIE	
		u_2	t_1	u_2	t_1	u_2	t_1	u_2	t_1	u_2	t_1	u_2	t_1
16	1.0[a]	0	288.54	26.30	220.61	3.80	289.08	4.08×10^8	171.78	-4.94×10^9	1113.98	−3.94	289.54
	2.0	0	144.27	1.10	148.64	3.81	144.52	9.56×10^8	−0.94	1.30×10^9	186.015	−2.49	142.27
48	1.0[a]	0	288.54	19.10	234.12	0.32	288.55	-8.68×10^8	834.96	-8.68×10^8	834.962	−0.52	289.53
	2.0	0	144.27	0.10	144.61	0.32	144.31	5.76×10^9	−1371.0	5.76×10^8	−1371.00	−0.52	144.27

[a] Degenerate scale.

Table 4
Numerical results for the potential problem with a multiply connected region by using the CHEEF concept

$2N$	R_2	Analytical solution		One interior point (0.5, 0)		One exterior point (4, 0)		One exterior point (5, 3)		Two exterior points (4, 0) (5, 3)		Two exterior points (4, 3) (7, 9)		One interior and one exterior point (0.5, 0.5) (4, 6)	
		u_2	t_1	u_2	t_1	u_2	t_1	u_2	t_1	u_2	t_1	u_2	t_1	u_2	t_1
16	1.0[a]	0	288.54	−7.1	363.2	1.9	286.9	1.7	287.5	1.6	287.9	1.5	288.2	−16.5	325.6
	2.0	0	144.27	1.5	146.5	1.6	146.8	1.5	146.3	1.7	145.7	1.6	145.3	1.5	145.9
48	1.0[a]	0	288.54	−35.5	395.8	0.12	288.49	0.11	288.51	0.11	288.53	0.11	288.53	−2.10	300.52
	2.0	0	144.27	0.11	144.61	0.11	144.56	0.11	144.53	0.11	144.56	0.11	144.54	0.11	144.51

[a] Degenerate scale.

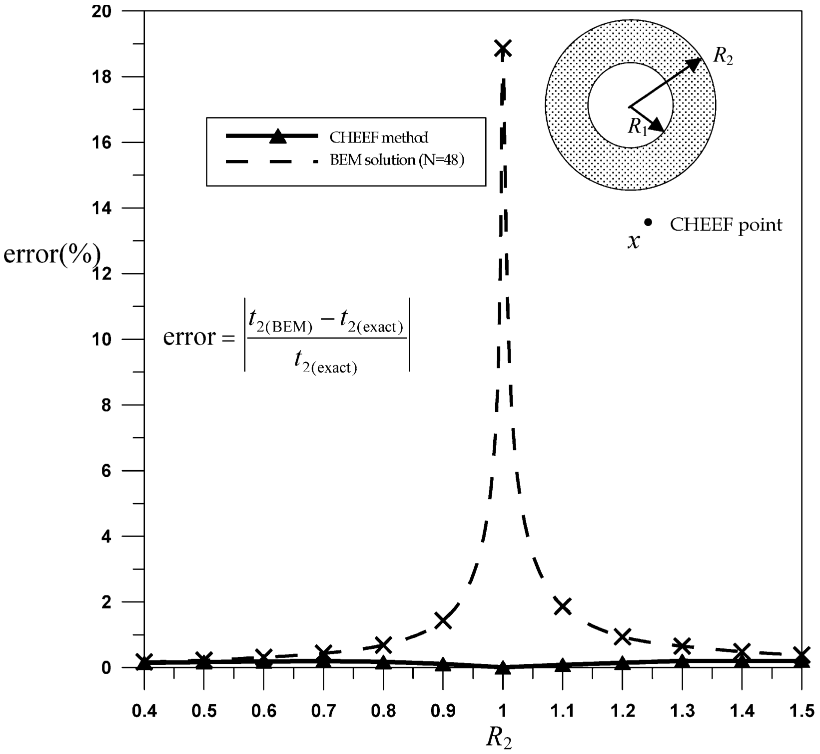

Fig. 6. The error of t_2 using different methods.

rank is deficient by only one and no zero is found in the complementary domain for the null-field solution.

Acknowledgments

Financial support from the National Science Council under Grant No. NSC-90-2211-E-019-003 for National Taiwan Ocean University is gratefully acknowledged. The authors thank Mr. S. R. Lin for providing the numerical results using a rigid body motion.

References

[1] Banerjee PK, Watson JO. Industrial applications of boundary element methods. New York: Elsevier; 1989.
[2] Cruse TA. Recent advances in boundary element analysis method. Comput Meth Appl Mech Engng 1987;62:227–44.
[3] Schenck HA. Improved integral formulation for acoustic radiation problems. J Acoust Soc Am 1968;55(1):41–58.
[4] Juhl P. A numerical study of the coefficient matrix of the boundary element method near characteristic frequencies. J Sound Vib 1994; 175(1):39–50.
[5] Chen JT. On fictitious frequencies using dual series representation. Mech Res Commun 1998;25(5):529–34.
[6] Chen IL, Chen JT, Liang MT. Analytical study and numerical experiments for radiation and scattering problems using the CHIEF method. J Sound Vib 2001;109(3):982–99.
[7] Christiansen S. Integral equations without a unique solution can be made useful for solving some plane harmonic problems. J Inst Math Appl 1975;16:143–59.
[8] Petrovsky IG. Lectures on partial differential equations. New York: Interscience; 1971.
[9] Jaswon MA, Symm GT. Integral equation methods in potential theory and electrostatics. New York: Academic Press; 1977.
[10] He WJ, Ding HJ, Hu HC. Non-equivalence of the conventional boundary integral formulation and its elimination for plane elasticity problems. Comput Struct 1996;59(6):1059–62.
[11] He WJ, Ding HJ, Hu HC. Degenerate scales and boundary element analysis of two dimensional potential and elasticity problems. Comput Struct 1996;60(1):155–8.
[12] He WJ, Ding HJ, Hu HC. A necessary and sufficient boundary element integral formulation for plane elasticity problems. Commun Numer Meth Engng 1996;12:413–24.
[13] He WJ. An equivalent boundary element integral formulation for bending problems of thin plates. Comput Struct 2000;74:319–22.
[14] Zhou SJ, Sun SX, Cao ZY. The boundary contour method based on the equivalent boundary integral equation for 2-D linear elasticity. Commun Numer Meth Engng 1999;15(11):811–21.
[15] Tomlinson K, Bradley C, Pullan A. On the choice of a derivative boundary element formulation using Hermite interpolation. Int J Numer Meth Engng 1996;39(3):451–68.
[16] Mitra AK, Das S. Nonuniqueness in the integral equations formulation of the biharmonic equation in multiply connected domains. Comput Meth Appl Mech Engng 1988;69:205–14.
[17] Chen JT, Lin JH, Kuo SR, Chiu YP. Analytical study and numerical experiments for degenerate scale problems in boundary element method using degenerate kernels and circulants. Engng Anal Bound Elem 2001;25:819–28.
[18] Chen JT, Lin JH, Kuo SR, Chyuan SW. Boundary element analysis for the Helmholtz eigenvalue problems with a multiply connected domain. Proc R Soc Lond A 2001;457:2521–46.
[19] Chen JT, Kuo SR, Lin JH. Analytical study and numerical experiments for elasticity plane problem with degenerate scale problems in boundary element method. Int J Numer Meth Engng 2002;54:1669–81.

[20] Kuhn G. Finite elements and boundary element techniques from mathematical and engineering point of view. In: Stein E, Wendland W, editors. BEM in elastostatics and fracture mechanics. International center for mechanical science (ICMS), courses and lectures, Berlin: Springer; 1988.
[21] Constanda C. On nonunique solutions of weakly singular integral equations in plane elasticity. Q J Mech Appl Math 1994;47:261–8.
[22] Constanda C. Integral equations of the first kind in plane elasticity. Q Appl Math 1995;53:783–93.
[23] Chen IL, Chen JT, Kuo SR, Liang MT. A new method for true and spurious eigensolutions of arbitrary cavities using the combined Helmholtz exterior integral equation method. J Acoust Soc Am 2001; 109(3):982–98.
[24] Chen JT, Wong FC. Analytical derivations for one-dimensional eigenproblems using dual BEM and MRM. Engng Anal Bound Elem 1997;20(1):25–33.
[25] Kuo SR, Chen JT, Huang CX. Analytical study and numerical experiments for true and spurious eigensolutions of a circular cavity using the real-part BEM. Int J Numer Meth Engng 2000;48:1401–22.
[26] Chen JT, Kuo SR, Chen KH. A nonsingular formulation for the Helmholtz eigenproblems of a circular domain. J Chin Inst Engng 1999;22(6):729–40.
[27] Stanley JF. Partial differential equations for scientists and engineers. New York: Dover; 1993.
[28] Chen JT, Kuo SR. On fictitious frequencies using circulants for radiation problems of a cylinder. Mech Res Commun 2000;27(1): 49–58.
[29] Chen JT, Chiu YP. On the pseudo-differential operators in the dual boundary integral equations using degenerate kernels and circulants. Engng Anal Bound Elem 2002;26:41–53.
[30] Chiu YP. A study on symmetric and unsymmetric BEMs. Master Thesis. Department of Harbor and River Engineering, National Taiwan Ocean University; 1999 (in Chinese).
[31] Moon P, Spencer DE. Field theory handbook. Berlin: Springer; 1961.